Path-entangled photon sources on nonlinear chips

Alexander S. Solntsev[1,*] and Andrey A. Sukhorukov[1]
[1]Nonlinear Physics Centre, Research School of Physical Sciences and Engineering,
Australian National University, Canberra, ACT 2601 Australia
*E-mail address: Alexander.Solntsev@anu.edu.au

July 19, 2017

Abstract

Photon entanglement has a range of applications from secure communication to the tests of quantum mechanics. Utilizing optical nonlinearity for the generation of entangled photons remains the most widely used approach due to its quality and simplicity. The on-chip integration of entangled light sources has enabled the increase of complexity and enhancement of stability compared to bulk optical implementations. Entanglement over different optical paths is uniquely suited for photonic chips, since waveguides are typically optimized for particular wavelength and polarization, making polarization- and frequency-entanglement less practical. In this review we focus on the latest developments in the field of on-chip nonlinear path-entangled photon sources. We provide a review of recent implementations and compare various approaches to tunability, including thermo-optical, electro-optical and all-optical tuning. We also discuss a range of important technical issues, in particular the on-chip separation of the pump and generated entangled photons. Finally, we review different quality control methods, including on-chip quantum tomography and recently discovered classical-quantum analogy that allows to characterize entangled photon sources by performing simple nonlinear measurements in the classical regime.

1 Introduction

Harnessing the unusual properties of quantum-entangled photonic systems facilitates the development of new technologies such as quantum computing [1], quantum communication [2], quantum-enhanced measurement [3] and quantum spectroscopy [4, 5]. Today the two most widely used approaches to generate quantum-entangled photons rely on nonlinear optical material response. Utilizing quadratic optical nonlinearity enables spontaneous parametric down-conversion (SPDC), a process in which a photon from a pump laser splits into two entangled photons traditionally named signal and idler [6, 7]. A similar process utilizing cubic nonlinear optical response called spontaneous four-wave mixing (SFWM) can destroy two pump laser photons to create a pair of entangled photons [7]. Both SPDC [8] and SFWM [9] can be employed for efficient squeezed light generation [10] above the pump power threshold, however in this review we focus on photon-pair generation below the threshold. In this case the efficiency of SPDC and SFWM has to be small to minimize the generation of higher photon number states, and is typically limited to about 10^{-5} pairs per one pump photon [9, 11], although it might be possible to increase it with multiplexing [12]. Despite relatively low efficiency, SPDC and SFWM offer near-unity indistinguishably and sub-GHz photon-pair rates [13], which makes them very attractive for a range of quantum information applications.

On-chip quantum photonics is a promising platform for the realization of these functionalities in compact and robust circuits suitable for both research and user applications [14, 15]. Integrating optical elements onto a single chip reduces the contact with the environment, preserving the fidelity of the quantum entanglement by suppressing phase fluctuations and other sources of noise [16]. Integrated devices are also compact and stable, so they can be combined to build complex quantum circuits that would be impossibly large using traditional bulk optics. Furthermore, integration avoids the complexity of coupling quantum states from free space to micro-scale waveguides, and makes the system more suitable for a range of practical applications outside the laboratory environment. On-chip SPDC was realized in periodically poled Lithium Niobate

(PPLN) waveguides [11, 17] and AlGaAs waveguides [18, 19], while SFWM was demonstrated with silicon on insulator (SOI) [20, 21, 22], chalcogenide glass [23, 24] and Hydex glass platforms [9]. The generation efficiency can be enhanced in ring resonators [9, 25, 26, 27, 28] and photonic-crystal waveguides based on slow light [29, 12, 30]. In the recent years many different kinds of entanglement have been demonstrated on a chip [31], including time-bin [32], time-energy [33], spectral [34] and path [35, 36, 37, 38] entanglement.

The concept of path entanglement provides a natural representation of quantum bits and more complex states in on-chip architectures, where the photons can be 'spread out' between multiple waveguides [39]. Coupling between waveguides can then serve as beam splitters, allowing the construction of quantum logic gates [16, 40, 41, 42, 43]. A range of quantum algorithms have been experimentally demonstrated, such as Shor's factoring algorithm [44], the integrated preparation and measurement of quantum states [45], quantum walks of entangled photons [46], Boson sampling [47, 48, 49, 50], and quantum teleportation [51]. Whereas most often the circuits are designed for photons with a fixed polarization, manipulation of polarization-entangled photons was also realized [52]. Several experimental works also focused on fiber-integrated approach as an intermediate step between bulk implementation and full on-chip integration [53, 54]. Finally, we note a recent demonstration of on-chip highly efficient superconducting photon detectors [55], and such technological advances open a way towards fully integrated quantum state measurement.

On-chip generation of path-entangled photons presents new challenges and opportunities associated with the spatial degree of freedom. In this paper, we present a review of the latest experimental demonstrations and theoretical proposals. In Sec. 2, we discuss the generation of path-entangled photons in coupled waveguides and approaches for all-optical tunability of the quantum states through shaping of the classical beam. Then in Sec. 3, we overview approaches of quantum state engineering through the modification of structural characteristics using thermal and electro-optic effects. In the following Sec. 4, we outline approaches for filtering out the strong pump from the generated few-photon states. We then discuss the methods of on-chip quantum state tomography (QST) in Sec. 5. We overview the application of classical nonlinear wave mixing for characterizing quantum performance of nonlinear chips, under realistic conditions including possible losses in Sec. 6. Finally, we present conclusions and outlook in Sec. 7.

2 Generation of path-entangled photons and all-optical tunability

Path entanglement (i.e. spatial entanglement) is intrinsically suitable for on-chip integration and is likely to play an important role in the future development of quantum optical technologies. In this approach multiple photon paths can be represented by different on-chip waveguides. The simplest system in which path-entangled photons can be generated is a coupler composed of two nonlinear waveguides.

In Ref. [38], the authors demonstrate how the flexibility of coupled waveguide systems can be harnessed for precise control of the process of photon-pair generation, enabling an on-chip biphoton source with wide quantum state tunability. To experimentally demonstrate this concept, they use two identical parallel waveguides with evanescent mode coupling as shown in Fig. 1(a), fabricated in $LiNbO_3$, a material with high second-order nonlinearity. Two waveguides are sufficient to generate path-entangled Bell states (states with maximum entanglement) and demonstrate wide-range tunability. Photon pairs are generated by spontaneous parametric down-conversion [56], where the properties of the generated pairs depend on the phase mismatch $\Delta\beta$ in the waveguides and on the pump. The signal and idler photons can be generated along the whole coupler, with probabilities of being generated at different points interfering between each other. The generated photons can also hop between the waveguides due to evanescent coupling with the coupling constant c, whereas the pump beams are confined to their excitation sites due to the strong confinement of the modes at pump wavelength [57]. Such a system has been shown to generate N00N states (a state which represents a superposition of N photons in mode a with zero photons in mode b, and vice verse) with $N = 2$ when pumped in one waveguide [58]. The coupler is driven by two classical pump beams, one coupled into each waveguide, with a variable phase difference $\Delta\varphi$ between them. Depending on the phase difference $\Delta\varphi$ and the phase mismatch $\Delta\beta$ various output states are possible [59].

The system of two coupled waveguides has two eigenmodes, symmetric (even) and anti-symmetric (odd), which have a phase difference of 0 or π, respectively, between the fields in the two waveguides. These

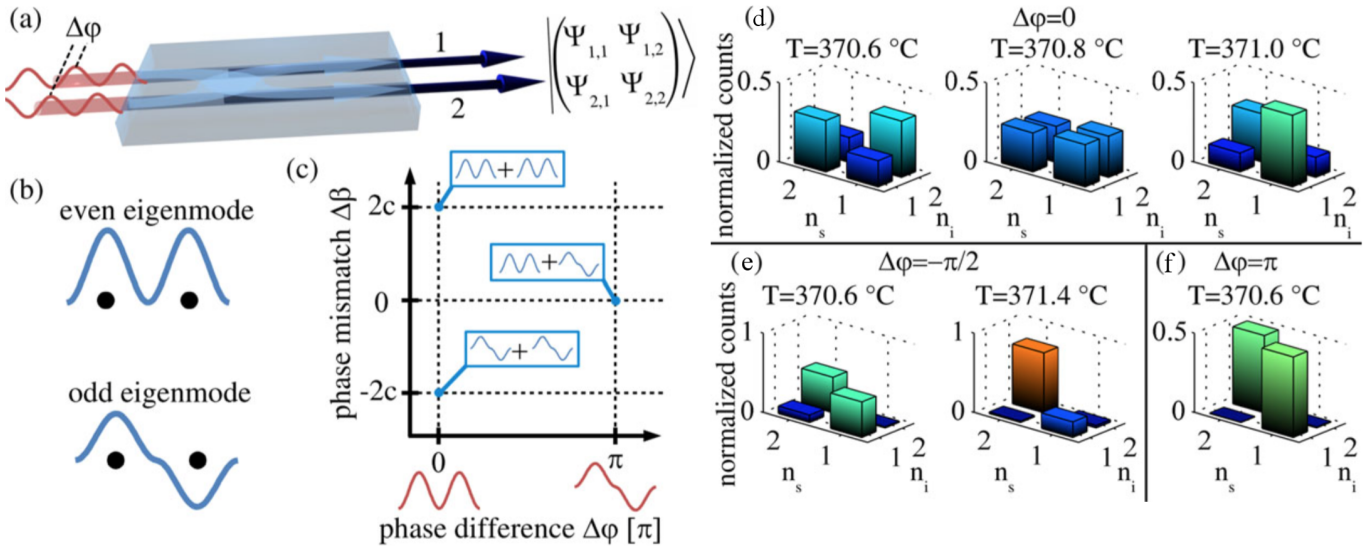

Figure 1: (a) Sketch of the scheme for tunable generation of biphoton quantum states, with two pump beams (red) exciting a directional coupler and generating photon pairs (blue) through SPDC. The output state is described by a wavefunction in the spatial basis. (b) Schematic representation of even (upper panel) and odd (lower panel) eigenmodes of the coupler, where the black dots denote the waveguide cores. (c) Parameter space of the phase mismatch and input phase difference where points of phase-matching to specific combinations of signal and idler eigenmodes are marked by the blue dots. (d-f) Normalized biphoton correlations for different output states. (d) Quantum state generation for $\Delta\varphi = 0$ and different phase mismatches $\Delta\beta$, showing the tunability from anti-bunching (left) to bunching (right). (e) Steering of photon pairs for $\Delta\varphi = -\pi/2$, from even distribution between output waveguides to predominant emission from waveguide 2. (f) Generation of bunched N00N-state for $\Delta\varphi = \pi$ (from Ref. [38]).

eigenmodes are schematically depicted in Fig. 1(b). By changing the pump phase difference, the pump can be continuously tuned between these two modes. SPDC depends on both the overlap of the pump, signal, and idler modes and the phase mismatch $\Delta\beta$, as schematically shown in Fig. 1(c). A variety of quantum states can be generated within the two-dimensional parameter space defined by $\Delta\beta$ and $\Delta\varphi$.

The output of the photon-pair source is characterized by correlation measurements over the two possible spatial positions of the photons. As shown in Fig. 1(d) the authors demonstrate output state tuning by changing the sample temperature for pump beams of equal phase. For a temperature of 370.6°C, corresponding to a phase mismatch of $\Delta\beta = 0$, strong anti-bunching (i.e. signal and idler photons exiting from opposite waveguides) is observed. With growing temperature and phase mismatch, an increasing amount of bunching (i.e. signal and idler photons exiting together from either waveguide) is measured, leading to a state with equal count numbers for all waveguide combinations and finally to dominant bunching. The authors mention that pure anti-bunching is difficult to achieve due to inhomogeneity of the sample. Steering of the generated photon pairs into just one waveguide occurs when the phase difference between two pump beams is $\Delta\varphi = -\pi/2$, which is shown in Fig. 1(e). Using pumps with $\Delta\varphi = \pm\pi$ leads to complete bunching of the generated photons depicted in Fig. 1(f). This output state corresponds to a 2-photon N00N-state, which is confirmed by full quantum state tomography [38].

Since a simple system of two coupled nonlinear waveguides provides such a widely reconfigurable platform for on-chip path-entangled photon-pair generation, it is important to understand SPDC in a larger number of coupled waveguides. As was shown in Ref. [35] experimentally and analyzed in details in Refs. [60, 61, 62, 63, 64, 65] theoretically, in an array with a large number of waveguides, photon pairs are continuously generated along the pump waveguide, as schematically illustrated in Fig. 2(a). While the pump beam stays in the input waveguide [66, 67], the generated photon pairs having approximately two times larger wavelength can couple to neighboring waveguides and undergo a quantum walk [46] (a quantum analogue of classical random walks), which due to interplay with the generation mechanism shapes the correlations towards the output state. The cascade of quantum walks in a waveguide array driven be the interference between probabilities to generate photon pairs at the different positions in the structure can be represented

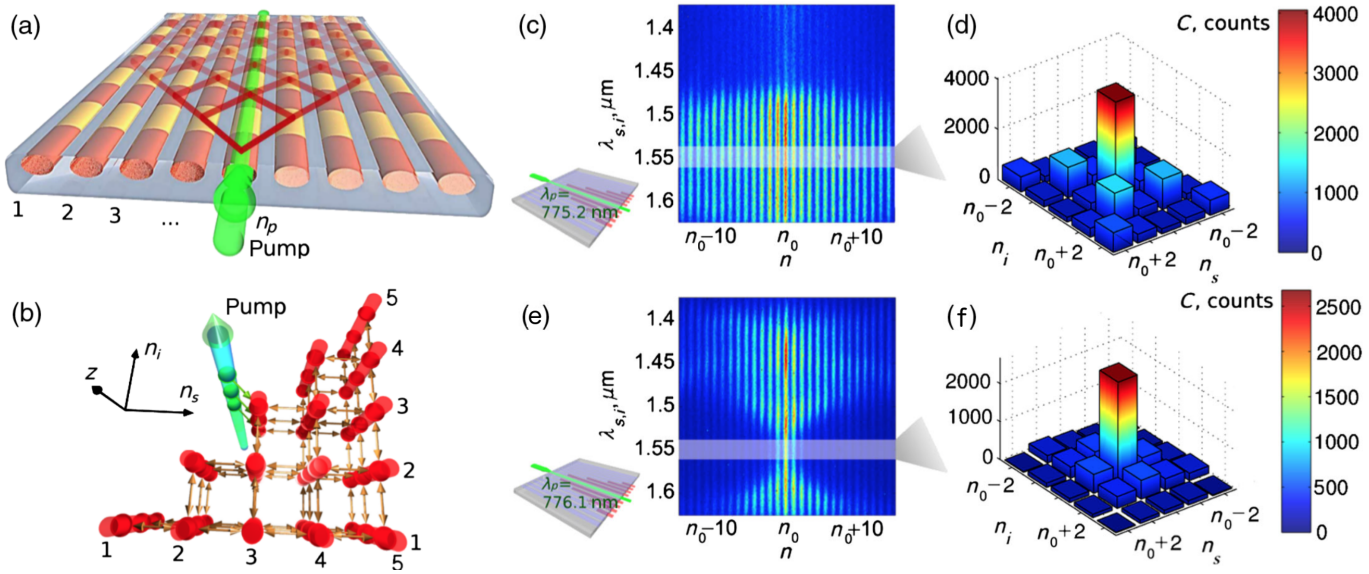

Figure 2: (a) Schematic illustration of a quadratic nonlinear waveguide array. The pump (green) is coupled to the waveguide number n_p. The photon pairs (red) are generated in the pump waveguide and propagate in the regime of quantum walks. (b) Representation of a photon-pair quantum walk on a lattice, where n_s and n_i are the signal and idler photon positions, respectively. A pump (green arrow) generates photon pairs continuously along the propagation direction z; signal and idler photons walk between waveguides (orange arrows). (c,e) Spatio-spectral photon-pair output distributions and (d,f) corresponding correlations using a spectral filter (gray area). The pump beam is coupled to a waveguide at the center of the array ($n_p = n_0$) with the pump wavelength (c,d) $\lambda_p = 775.2$ nm and (e,f) $\lambda_p = 776.1$ nm (from Ref. [35]).

as a multi-level graph schematically shown in Fig. 2(b). Here, a linear quantum walk of the generated photon pair is visualized with a red two-dimensional (2D) grid, where n_s and n_i denote the positions of signal and idler photons. Each 2D grid represents a two-dimensional quantum walk, which is similar to the walks studied before in linear waveguide arrays [46].

The results of spatio-spectrally resolved classical intensity measurements of the SPDC output in a $LiNbO_3$ waveguide array are depicted in Fig. 2(c). They show one broad spectral maximum of the generated photon pairs around a wavelength of $2\lambda_p = 1550.4$ nm, very close to the wavelength of degenerate photon pairs which is 1550.5 nm. The resulting coincidence counts for the degenerate pairs are shown in Fig. 2(d), demonstrating pronounced simulations spatial bunching and anti-bunching. For a shifted pump wavelength, the highest SPDC intensities are achieved for offset signal and idler wavelengths of 1450 nm and 1670 nm, indicating non-degenerate SPDC, shown in Fig. 2(e). The results of correlation measurements for this pump wavelength and photon-pair wavelength filtering around the degenerate regime [gray shading in Fig. 2(e)] are presented in Fig. 2(f), again showing a dominating contribution from the $\{n_0, n_0\}$ position corresponding to the pumped waveguide. However, in contrast to the case described above, no pronounced bunching and anti-bunching in other waveguides is observed. The theoretical analysis performed in Ref. [35] shows that the state with the correlations shown in Fig. 2(d) incorporates large scale path entanglement. It is also important to mention that path-entangled biphoton generation in waveguide arrays is tolerant to significant losses, as completely destroying the entanglement requires losses to be strong enough to prevent the coupling between the waveguides [69]. Furthermore, the same system can also be used for spectral entanglement generation [70].

These results demonstrate that an array of nonlinear coupled waveguides represents a very promising system for the generation of large-scale spatial entanglement with controllable spatial correlations. The next step in the evolution of the quantum optical sources based on the coupled nonlinear waveguides is tailoring their properties to generate arbitrary useful path-entangled states. In Ref. [68] the authors predict that a photonic chip consisting of an array of coupled nonlinear waveguides can be designed for all-optically controlled generation of any set of path-entangled biphoton states. This device is particularly elegant

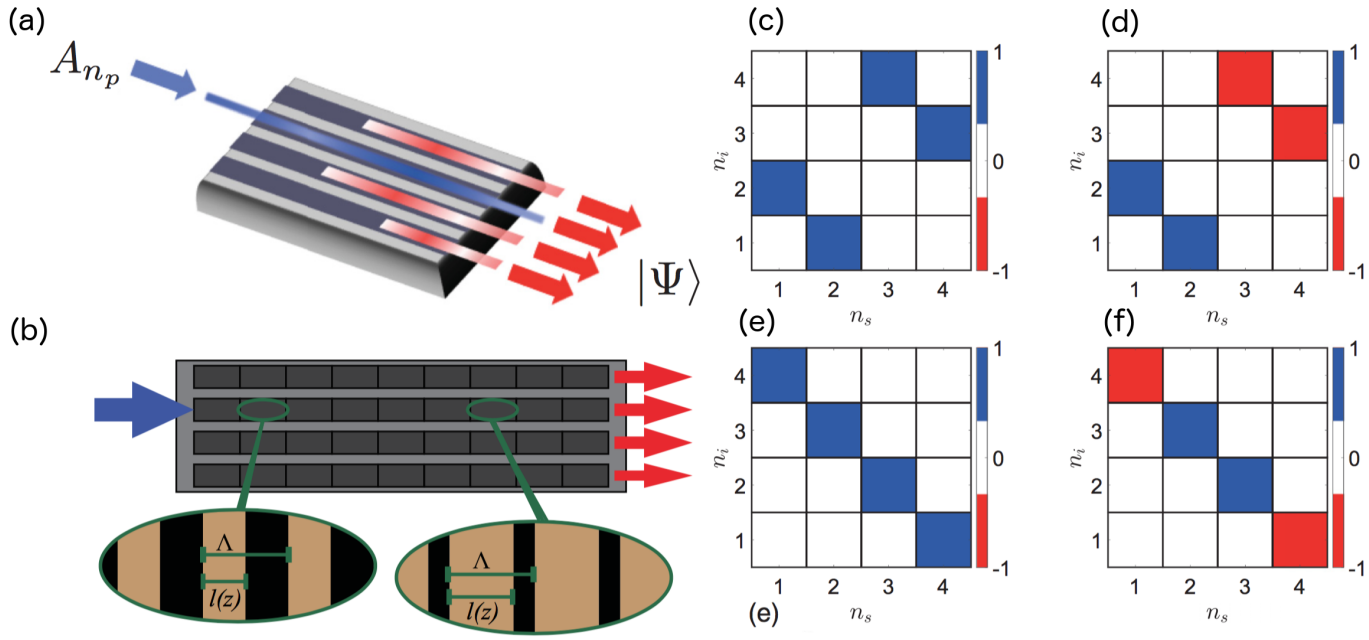

Figure 3: (a) Diagram of a nonlinear waveguide array. A pump laser field, A_{n_p} (leftmost arrow) drives a waveguide in the nonlinear waveguide array. The interaction between the laser and the $\chi^{(2)}$ nonlinearity of the waveguide produces entangled photons (red arrows on right side) via SPDC. These entangled photons can couple into neighboring waveguides, producing path-entangled states, Ψ, at the output. (b) Top view of the array. Each waveguide is divided into a number of segments, with different aggregate values of second order nonlinearity. The aggregate nonlinearity is controlled by varying the ratio of up-to-down poling (the duty cycle) of the nonlinear crystal. This provides control of the photon-pair wavefunction. (c),(d),(e),(f) Target output biphoton states produced when each of the four waveguides is pumped individually. The states are equivalent to Bell states using dual-rail encoding [45], where the signal photon occupying waveguide 1(3) represents a logical 0(1) and similarly for the idler photon in waveguides 2 and 4 (from Ref. [68]).

because the output quantum wavefunction is directly mapped from the amplitudes and phases of the classical laser inputs. Hence the device can be reconfigured in real time by varying classical inputs, providing a flexible interface between classical and quantum information. The device concept is demonstrated in Fig. 3(a). The authors demonstrate that the nonlinear waveguide array could be tuned to produce custom and reconfigurable quantum states, which can be achieved through specially designed domain poling, as shown in Fig. 3(b). To illustrate this general approach they design a four-waveguide device with poling to generate the set of two-photon Bell states as the outputs [Fig. 3(c)-(f)]. Ref. [68] also provides detailed analysis of the sensitivity of this approach to fabrication inaccuracies.

To summarize, coupled nonlinear waveguides can be used to generate photons with path entanglement and provide wide-range all-optical tunability of the generated states. The systems discussed above utilized $LiNbO_3$ waveguides with the length of several cm and the corresponding photon-pair generation efficiencies on the order of 10^{-7} for sub-mW range continuous-wave pump. The photon-pair rates in the MHz range were limited by the coupling to the single-photon detectors and their speed and quantum efficiency [35, 38]. In the next section we focus on other ways of achieving photon-pair source tunability.

3 Electro- and thermo-optical tunability

In the previous section all-optical tunability of on-chip generated photon pairs was discussed. Alternative ways to tune the photon-pair correlations and entanglement are based on electro-optical and thermo-optical effects.

In Refs. [36] the authors present a photon-pair source with thermo-optical tunability based on SOI platform. The platform benefits from widespread use of silicon lithography and small footprint. The SOI

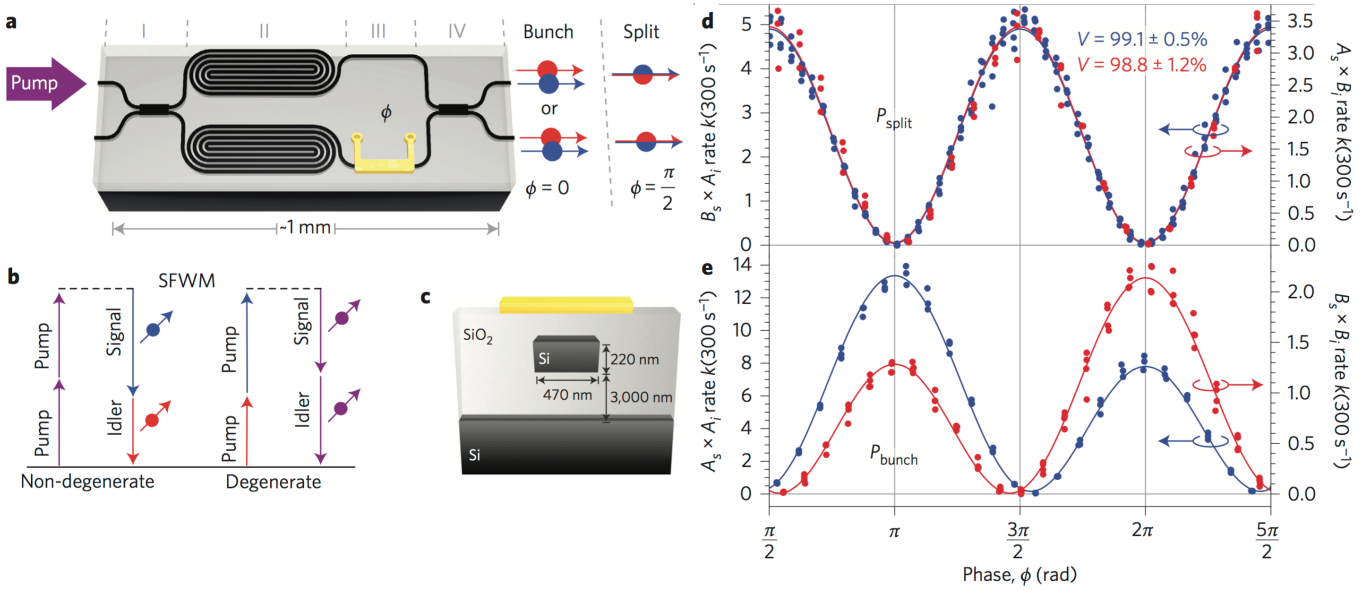

Figure 4: (a) Scheme of the device operation. A bright pump laser is coupled to the SOI chip using a lensed optical fiber and on-chip spot-size converters (not shown). The pump is distributed between two modes via a 2 x 2 MMI coupler (I), and excites the $\chi^{(3)}$ SFWM effect within each spiral SOI waveguide source (II) to produce signal–idler photon pairs in the two-photon entangled state $(|2,0> -|0,2>)/\sqrt{2}$. The pairs are thermo-optically phase shifted (ϕ, III) and interfered on a second coupler (IV) to yield either bunching or splitting over the two output modes, depending on ϕ. (b) Energy diagrams of both types of SFWM, showing the time-reversal symmetry between the non-degenerate and degenerate processes. (c) SOI waveguide cross-section, with the thermal phase shifter on top. (d) Measurement of signal–idler photon splitting between modes A and B, showing quantum interference. (e) Measurement of signal–idler photon bunching, with signal and idler both in mode A or mode B. Fringe asymmetry arises from spurious SFWM pairs generated in the I/O waveguides (from Ref. [36]).

photonic device is presented in Fig. 4(a). Inside the device there are two photon-pair sources, each of which comprises a spiral silicon waveguide 5.2 mm long optimized for the spontaneous four-wave mixing process [region II, Fig. 4(a)]. SFWM creates a signal–idler photon pair by annihilating two photons from a bright pump beam (Fig. 4(b)). Non-degenerate pairs are created by a single-wavelength pump, and degenerate pairs require a dual-wavelength scheme [71]. In this experiment, two amplified continuous-wave lasers produced the required pump field. Pump distribution and single-photon interference were achieved using 2 x 2 multimode interference (MMI) couplers, and a thermal phase shifter modified the on-chip quantum and bright-light states. Off-chip wavelength-division multiplexers (WDMs) were used to separate the signal, idler and pump channels before the photon pairs were finally measured by two superconducting single-photon detectors. Fig. 4(c) shows SOI waveguide cross-section, with the thermal phase shifter on top.

Evolution of the degenerate quantum states proceeded as follows [Fig. 4(a), regions I–IV]. The bright pump was split equally by the first MMI coupler (I) between the two sources (II). By operating in the weak pump regime (so that only one pair was likely to be generated), the simultaneous pumping of both sources yielded a path-entangled N00N state, $(|2,0> -|0,2>)/\sqrt{2}$. The relative phase was then dynamically controlled via a thermal phase shifter in one arm (III), which applied a ϕ shift to the bright-light pump and a 2ϕ shift to the entangled biphoton state, $(|2,0> -\exp[-2i\phi]|0,2>)/\sqrt{2}$. Finally, the bright-light and biphoton states were interfered on a second MMI coupler (IV) to yield Mach–Zehnder interference fringes. The measurements for the photon-pair bunching rate and splitting rate are shown in Fig. 4(d) and Fig. 4(e), respectively. For the bunching rate, an asymmetric behavior is observed. This can be explained by considering spurious SFWM pairs in the device's input and output (I/O) waveguides, identical in cross-section to the source waveguides [Fig. 4(c)].

The approach of thermal tuning was also applied to generate indistinguishable photons from two on-chip ring resonators, compensating for mismatch between the rings due to fabrication imperfections [72]. It was shown that such sources are suitable for creation of entangled qubits, as confirmed with on-chip tomography

integrated on the same chip. The tomography circuit also employed thermo-optic elements to realize variable phase shifts.

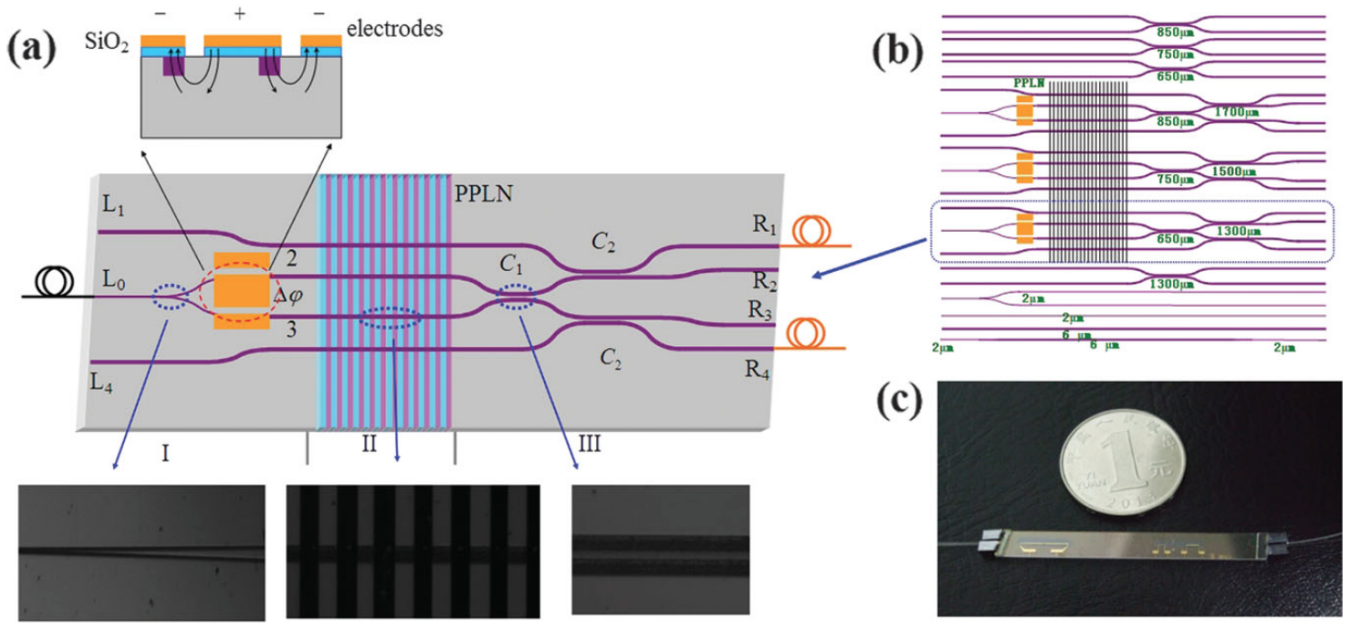

Figure 5: (a) The photonic chip with dimensions of 50 mm x 5 mm x μm for the pump and 6 μm for entangled photons. The periodically poled section is 10 mm long with a period of 15.32 μm. The interaction length of C_1 / C_2 is 650 μm / 1300 μm at a gap of 4 μm. The upper inset is the structure of the electro-optic modulator. The electrode pairs are 8.35 mm long with a separation of 6 μm. The buffer layer (SiO_2) is etched along the gap between the electrodes to suppress dc drift. The lower three insets are the micrographs of the Y branch, the PPLN waveguide, and the directional coupler, respectively. (b) The whole structure of the chip. (c) Photograph of the chip with fixed fiber pigtails (from Ref. [37]).

Electro-optical tunability presents another approach to tunable photon-pair sources, as suggested theoretically in Ref. [73] and demonstrated experimentally in Ref. [37]. Figure 5(a) shows the main structure of the chip. Basically, it is composed of annealed proton exchanged channel waveguides integrated on a Z-cut PPLN crystal. This design enables the generation, interference, and filtering of entangled photons from separate regions of PPLN waveguides, leading to reconfigurable on-chip quantum light sources. The chip can be characterized by three sections. Section I is designed to deal with the classical pump light. A 780 nm pump is coupled into waveguide L_0 and equally distributed by a Y-branch single mode beam splitter at the wavelength of 780 nm. After the Y branch, the electro-optic effect is used to control the phase shift between two paths. Electrodes are fabricated above two pump waveguides for applying a voltage. Transition tapers connect the 780 nm Y branch with the 1560 nm single mode waveguides. Section II is the PPLN region, in which degenerate photon pairs at 1560 nm are generated through SPDC indistinguishably from either one of the two PPLN waveguides, yielding a path-entangled state $(|2,0> - \exp[-2i\phi]|0,2>)/\sqrt{2}$. The relative phase ϕ is transferred from the phase difference of pump modes. In section III, quantum interference is realized by a 2 x 2 directional coupler (C_1). The on-chip phase is adjusted by changing the voltage applied in section I. The entangled photons are separated from the pump by on-chip wavelength filters (C_2). Entangled photons are transferred to the neighboring waveguides R_1 and R_4. The pump is left in R_2 and R_3. The input waveguide L_0 and output waveguides R_1 and R_4 are directly connected with optical fiber tips, which are fixed with the chip by using UV-curing adhesive after reaching a high coupling efficiency. This removes the need for optimizing the coupling during the observation of quantum interference. As shown in Fig. 5(b), the lithium niobate chip contains three main photonic circuits, and each one has a structure similar to Fig. 5(a), the difference lying among three main circuits is the interaction lengths of C_1 and C_2. Figure 5(c) shows a photograph of the chip with fixed fiber pigtails. The experimental results of photon-pair generation and tuning presented in Ref. [37] closely resemble the degenerate case of the SOI chip discussed

above [36], see Fig. 4(d,e).

To summarize, there are various on-chip platforms enabling the generation of photon pairs with tunable path entanglement. $LiNbO_3$ has high quadratic susceptibility, and allows efficient spontaneous parametric down-conversion with fast electro-optical control. SOI systems allow the generation of photon pairs based on spontaneous four-wave mixing with slightly slower but still effective thermo-optical tuning. In both thermo-optical [36] and electro-optical [37] cases a voltage of 2 to 4 V was required for noticeable phase shifts. Although the above papers did not discuss switching speed, typical integrated thermo-optical and electro-optical switching can reach GHz rates. Moreover, as was discussed in the previous section, utilizing waveguides that are coupled and generate photon pairs along the whole propagation, allows using all-optical tunability that is fast and provides a wide quantum state tuning range [35, 38]. In terms of comparing the figures of merit, the generation of tunable path-entangled photon pairs in $LiNbO_3$ waveguides achieved 10^{-7} efficiency in cm-size footprint, while SOI platform reduced the footprint to sub 100 μm scale at the cost of decreasing the efficiency to 10^{-12} photon pairs per pump photon and requiring a pulsed pump. However ultimately both SPDC- and SFWM-based approaches can demonstrate small footprint coupled with high efficiency, as was shown by a variety of on-chip systems not featuring path entanglement [9, 11, 19, 22].

4 Pump filtering

In the previous sections we looked at the generation and tuning of path-entangled photon pairs on a chip. However before these biphotons can be measured in order to be used for various applications in quantum information, it is important to separate strong pump laser from the generated photons. There are multiple well-established ways to do it off the chip, mostly relying on spectral filtering using bulk optics [35, 38] and fibers [36]. However implementing pump filtering on a chip is more challenging and was only demonstrated recently.

Integrated photon-pair generation and pump filtering was demonstrated on a PPLN chip [37] which design was discussed in the previous section. The measured pump suppression was 29.2 dB for R_1 and 31.4 dB for R_4 ports where the photon pairs were collected as shown in Fig. 5(a). However further suppression of the pump was required, which was performed by interference filters centered at 1560 nm inserted into the fiber delay lines.

In Ref. [26] the authors show the generation of quantum-correlated photon pairs combined with the spectral filtering of the pump field by more than 95 dB on a single silicon chip using electrically tunable ring resonators and passive Bragg reflectors. The source components are shown in Fig. 6(a). Photon-pair generation takes place in an electrically tunable ring resonator via SFWM [74, 28, 25, 75]. A first stage of pump rejection by approximately 65 dB is achieved using a notch filter implemented by a 2.576-mm-long distributed Bragg reflector (DBR) consisting of a corrugated waveguide [76]. Signal and idler photon demultiplexing is performed using add-drop microring resonators. In an experiment performed on a single chip, two thermally tunable add-drop ring resonators are used to filter the remaining pump light, thereby totaling close to a 100-dB extinction ratio. At the output of the chip, the pump power is less than 1/10 of the combined signal and idler fields. In Ref. [77] cascaded lattice filters implemented on SOI platform were also able to provide over 100 dB pump extinction.

Another approach to on-chip pump filtering is based on photonic crystal structures. In Ref. [78] the authors propose a photonic crystal coupled-cavity system designed such that the coupling of the pump mode to the output channel is strictly zero due to symmetry. They further analyze this effect in presence of disorder and find that suppression close to 40 dB can be achieved with state-of-the art fabrication. Due to the small mode volumes and high quality factors, the photonic crystal system is expected to have a generation efficiency much higher than in standard micro-ring systems. The proposed design is based on a photonic crystal made of a triangular lattice of circular holes in a silicon slab suspended in air [Fig. 6(b)]. The thickness is kept as a free parameter, but the design is such that for the standard thickness of 220 nm of the silicon slab, the operational wavelength is in the telecommunication window around 1550 nm. For the resonant four-wave mixing, three identical cavities are introduced, as shown by three white areas in the middle of Fig. 6(b). The crucial observation that enables the pump filtering is based on the symmetry of

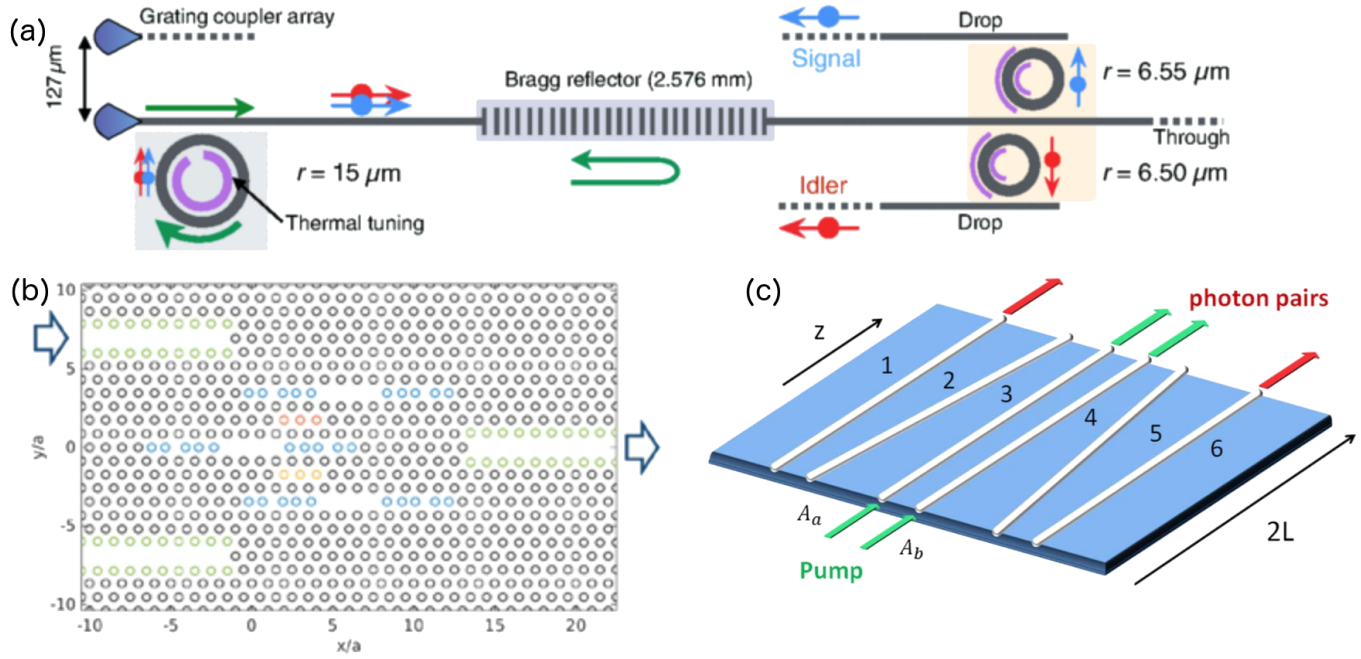

Figure 6: (a) Schematic layout of the photonic integrated circuit composed of a high-Q thermally tunable ring for efficient pair generation by spontaneous four-wave mixing, followed by a DBR for pump rejection and the add-drop ring-resonator filters for the demultiplexing of signal and idler photons (from Ref. [26]). (b) The proposed photonic crystal device for resonant spontaneous four-wave mixing. Arrows denote input (left) and output (right) channels for the three-cavity system. The geometry ensures that no power is radiated into the output waveguide at the pump frequency (from Ref. [78]). (c) Scheme of adiabatically coupled waveguiding structure: pump beams (green) are coupled to the central waveguides 3 and 4, and the Bell states (red) are formed in the edge waveguides 1 and 6 that are separate from the pumped waveguides (from Ref. [59]).

the structure with respect to reflection in the xz-plane. The three modes supported by the structure have eigenvalues -1, 1, and -1 with respect to the xz-reflection operator. Based on these symmetries, the authors show that full filtering of the pump mode can be achieved when the output channel does not support modes of the corresponding symmetry.

The pump filtering methods discussed above require state-of-the art fabrication precision. Another approach significantly more robust to fabrication inaccuracies is based on adiabatic pump filtering. In Ref. [59] the authors present an integrated scheme for generation of Bell states, which allows simultaneous spatial filtering of pump photons. It is achieved through spontaneous parametric down-conversion in the system of nonlinear adiabatically coupled waveguides. Analytic study reveals the optimal conditions for the generation of each particular Bell state, and numerical simulations of the device under realistic assumptions show that adiabatic coupling allows spatially filtering of the pump from modal-entangled photon pairs. Fig. 6(c) illustrates the proposed structure consisting of two adiabatic couplers (waveguides 1,2,3 and 4,5,6), where generated photons can also couple between the central waveguides. By designing the coupling strength of the waveguides, the SPDC phase mismatch, and the pump amplitudes in the two central waveguides, different spatially entangled bi-photon states can be obtained, and the generated photon pairs exit through waveguides 1 and 6. At the same time, the pump remains localized in the central waveguides 3 and 4. To estimate the performance of a realistic structure, the numerical calculations were performed of the coupling strength depending on the wavelength and the separation distance between the waveguides with COMSOL Multiphysics using parameters obtained in experiment [79]. They confirm that the coupling for the proposed 6-waveguide structure can be achieved for biphotons with the wavelengths around 1550 nm, and the adiabatic coupling configuration can provide the pump filtering of 72 dB. It can be further improved to reach the values exceeding 100 dB by adding an extra set of adiabatic passages in a 10-waveguide configuration. Importantly, adiabatic coupling is tolerant to substantial fabrication errors and works in a very broad range of over 400 nm in the telecom band [80]. As long as higher order pump modes are excluded, the pump filtering based

on adiabatic coupling presents a promising solution.

Overall, the approaches for integrated pump filtering can then enable on-chip generation and measurement of single photons. This would open new possibilities for device development with a variety of applications.

5 Quantum state tomography

In order to characterize the properties of an on-chip path-entangled photon source as well as to read out the results of quantum information experiments, a robust integrated approach to quantum state tomography in path basis is required.

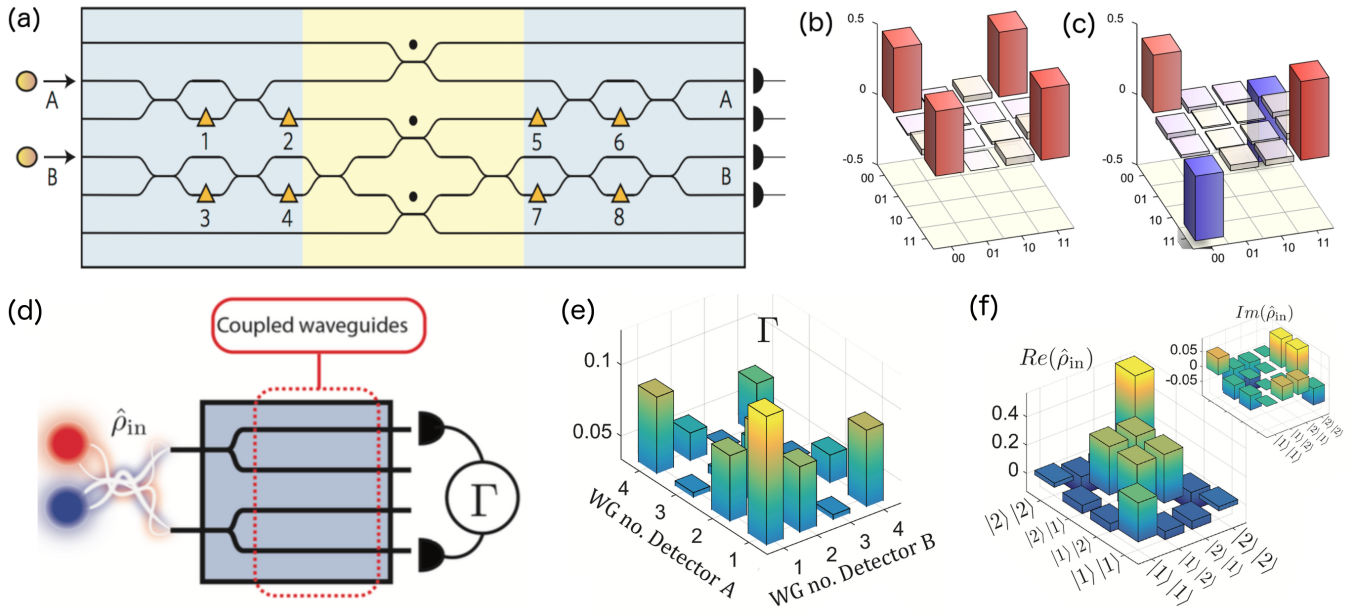

Figure 7: (a) Waveguide implementation of the two-photon reconfigurable quantum circuit for preparing, manipulating and detecting entanglement and mixture, composed of directional couplers and voltage-controlled thermo-optic phase shifters (marked as orange triangles). Directional couplers with splitting ratio of 1/3 are marked as dots; all other couplers have the splitting ratio of 1/2. The third blue shaded segment is used to implement quantum-state tomography. (b,c) Real parts of the density matrices of two different Bell states prepared and characterized on the chip. (from Ref. [45]). (d) Diagram of a hybrid quantum walk for two-photon tomography. A linear optical transformation operates on a mixed two photon state, then correlations between the photons are measured. The measured spatial photon correlations at the output of a specially tailored discrete-continuous quantum-walk can enable full reconstruction of any two-photon spatially entangled and mixed state at the input. This approach does not require any tunable elements, so is well suited for integration with on-chip superconducting photon detectors. (e) Simulated correlation measurements at the output of the circuit. (f) Real and imaginary parts of the input density matrix, recovered using correlation measurements shown in (e) (from. Ref. [81]).

In Ref. [45], the authors report an integrated waveguide device that can prepare and completely characterize pure two-photon states with any amount of entanglement and arbitrary single-photon states with any amount of mixture. The device consists of a reconfigurable integrated quantum photonic circuit with eight voltage-controlled phase shifters. It was demonstrated that, for thousands of randomly chosen configurations, the device performs with high fidelity. Preparation of maximally and non-maximally entangled states, violation of a Bell-type inequality with a continuum of partially entangled states, and demonstration of the preparation of arbitrary one-qubit mixed states were reported. The device shown in Fig. 7(a) is a silica-on-silicon (SOI) entangling circuit. Two photonic qubits A and B are encoded in pairs of waveguides – path or dual-rail encoding. The two qubits are input in the logical zero state (that is, a single photon in each upper waveguide) and are then acted upon by the quantum circuit shown in Fig. 7(a). The first part of

this circuit enables arbitrary state preparation of each qubit. The central part of the circuit implements a maximally entangling post-selected controlled-NOT (CNOT) logic gate (the canonical two-qubit entangling gate). The CNOT gate is a post-selected linear optical gate that works with probability 1/9 [82]. The final stage of the circuit is the mirror image of the first stage and is followed by measurement in the computational basis, which together enables projective measurement of each qubit in an arbitrary basis. This final stage can be used in various circuits enabling full on-chip quantum tomography. As an example, Figs. 7(b,c) show the real parts of the reconstructed density matrices (i.e. complete quantum descriptions) of two different path-entangled Bell states.

Another approach does not require reconfigurable phase-shifters. In Ref. [81] the authors show that reconfiguring the measurement setup is actually not necessary for quantum state tomography. They establish that one specially chosen static measurement setting is sufficient to fully characterize unknown density matrices. This insight means that the usually complex and error sensitive tomography process is simplified and noise introduced when reconfiguring the measurement setup is avoided. The method is inspired by compressed sensing. Conventionally in compressed sensing it is assumed that a signal is sparse in some basis, and this knowledge allows reconstruction of the signal from fewer measurements. This can be exploited for fast tomography of near pure quantum states [83] and quantum process tomography [84]. In Ref. [81] the unknown input state is transformed to become sparse, and then a compressed sensing-like approach to tomography is used. This is achieved by applying a linear transformation to the system that maps it to an increased number of modes, thus turning it into a sparse system. Careful choice of this transformation allows imaging of the full complex-valued density matrix just from measuring one set of expectation values after the transformation. Thus the mixed quantum state can be fully characterized with a static measurement setup. A linear optical circuit implementing this scheme is shown in Fig. 7(d). Here two input waveguides are split into an array of four, introducing sparsity. Following this, the four waveguides form a coupled waveguide array. This circuit allows quantum state tomography just by taking correlation measurements at the output. A simulated example of such correlation measurement Γ is shown in Fig. 7(e). Using the algorithm detailed in Ref. [81] this correlation measurement allows the reconstruction of both real and imaginary parts of the input density matrix $\hat{\rho}_{in}$ as shown in Fig. 7(f).

Characterization of states with more than two photons is important, but also more challenging and call for the development of new conceptual approaches. Recently, it was predicted that knowing that a quantum state is sparse can facilitate characterization of three-photon quantum states just by measuring two-photon coincidences [85]. Furthermore, coupled waveguide array platform was used to determine non-classicality of multi-photon states [86]. However, full on-chip tomography with reconstruction of multi-photon entanglement remains an open problem.

6 Quantum-classical correspondence

Measuring density matrices through full quantum state tomography or even just performing photon correlation measurements is time consuming, since statistics from a large number of photon counts has to be accumulated. When a fabricated nonlinear photonic chip needs to be characterized quickly to assess the quality of the fabrication, the best way to do it is by using quantum-classical correspondence. It relies on the fact that the biphoton wave function for a quantum source is precisely the response function for a classical field generated by the same device and input field, with an appropriate additional input seed field [87]. It allows direct but slow coincidence-detection measurements of a spontaneous process to be supplanted by faster and more convenient optical power measurements of the corresponding classical process. This measurement technique has enabled previously unobtainable resolution in the spectral characterization of two-photon states from various waveguides including an AlGaAs ridge waveguide [88] and a silicon nano-waveguide [89]. It has also facilitated a simple and efficient polarization-density matrix reconstruction method [90]. It is shown in Refs. [91, 92] that a difference-frequency generation (DFG) experiment gives information about an SPDC experiment in the same device for arbitrary SPDC pump spectral width if losses are either small or approximately equal for all interacting fields. Alternatively, a sum-frequency generation (SFG) experiment gives useful information for arbitrary losses provided the interacting waves are quasi-continuous [see

Fig. 8(a)]. Systems with cubic nonlinear optical response rely on the correspondence between spontaneous and stimulated four-wave mixing [87, 89].

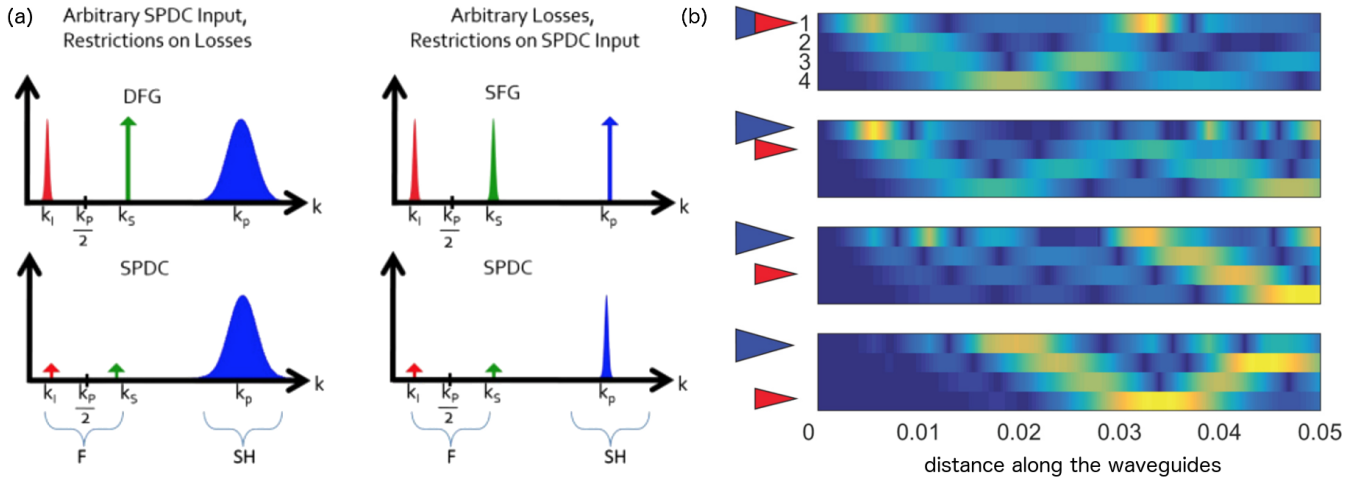

Figure 8: (a) Sketch of connections between input fields (Gaussians) and generated fields (arrows) for various second-order nonlinear optical processes (from Ref. [92]). (b) Signal field intensity evolution along the coupled waveguides in a waveguide array in the process of DFG. The larger arrow points to the pumped waveguide, while the smaller arrow denotes the seeded waveguide. Measuring the signal outputs generated by all combinations of pump and idler inputs allows to predict SPDC (from Ref. [68]).

In Ref. [68] this approach is extended to on-chip path entanglement. The authors show how to use classical DFG to determine the quantum wavefunction that would be produced by SPDC in an array of aperiodically poled waveguides. This approach requires inserting pump and idler fields in all combinations of waveguide inputs and measuring amplitudes and phases of the generated signal from all waveguide outputs [see Fig. 8(b)]. In Ref. [93] the authors show that phase measurements are not required if DFG is replaced with SFG, which they confirm experimentally. Thus, classical nonlinear optical processes can be used to quickly and efficiently characterize on-chip integrated photon sources with path entanglement, even in the cases of inhomogeneous nonlinearity or the presence of losses [94].

7 Outlook

Quantum information science and technology with photons will require circuits that are complex, stable and highly reconfigurable in a straightforward manner. High-fidelity production and measurement of states of arbitrary entanglement will be essential for the functioning of quantum devices, and will provide a reliable means with which to test the unique properties of quantum physics.

The inherent interferometric stability of integrated optics makes path-encoding of qubits a natural choice, while on-chip polarization encoding requires special designs [52, 95]. The path-encoding also enables efficient representation of higher-dimensional qudits [96]. This is in contrast with bulk optics, where two-level polarization encoding is more natural, and stable path encoding requires a considerable resource overhead [97]. Furthermore, path-entanglement could be used to enable encoding with multiple degrees of freedom combining path and polarization [98]. Time-bin entanglement [32], time-energy entanglement [33] and spectral entanglement [34] present other promising approaches to on-chip integration of quantum optical sources, providing more degrees of freedom in which photons can be entangled. It would be of particular interest to expand the hybrid path-time entanglement studied in bulk [99] to integrated photonic chips.

In terms of platforms, path-entangled on-chip photon sources have mostly utilized SOI and $LiNbO_3$ waveguides so far. The recent demonstrations include photon sources with thermo-optical [36], electro-optical [37] and all-optical [35, 38, 68] tunability, as well as means to filter out the pump [26, 78, 59] and characterize the performance using quantum [45, 81] and classical approaches [92, 88]. Other promising directions include utilizing AlGaAs, a material with high quadratic susceptibility and developing nano-

fabrication capabilities [18, 19], as well as replacing coupled waveguides with ring- or disk-resonators to reduce the footprint [72, 74, 28, 25, 75]. These approaches have demonstrated very efficient on-chip photon-pair generation, and utilizing them for path entanglement is of significant interest.

Acknowledgements

This work was supported by the Australian Research Council, including Discovery Projects DP130100135 and DP160100619.

References

[1] P. Kok, W. J. Munro, K. Nemoto, T. C. Ralph, J. P. Dowling, G. J. Milburn, Linear optical quantum computing with photonic qubits, Rev. Mod. Phys. 79 (1) (2007) 135–174. doi:10.1103/RevModPhys.79.135.
URL http://dx.doi.org/10.1103/RevModPhys.79.135

[2] N. Gisin, G. G. Ribordy, W. Tittel, H. Zbinden, Quantum cryptography, Rev. Mod. Phys. 74 (1) (2002) 145–195. doi:10.1103/RevModPhys.74.145.
URL http://dx.doi.org/10.1103/RevModPhys.74.145

[3] V. Giovannetti, S. Lloyd, L. Maccone, Quantum-enhanced measurements: Beating the standard quantum limit, Science 306 (5700) (2004) 1330–1336. doi:10.1126/science.1104149.
URL http://dx.doi.org/10.1126/science.1104149

[4] D. A. Kalashnikov, A. V. Paterova, S. P. Kulik, L. A. Krivitsky, Infrared spectroscopy with visible light, Nature Photonics 10 (2) (2016) 98+. doi:{10.1038/NPHOTON.2015.252}.

[5] A. S. Solntsev, G. K. Kitaeva, I. I. Naumova, A. N. Penin, Characterization of aperiodic domain structure in lithium niobate by spontaneous parametric down-conversion spectroscopy, Laser Physics Letters 12 (9) (2015) 095702.
URL http://stacks.iop.org/1612-202X/12/i=9/a=095702

[6] D. Klyshko, Physical Foundations of Quantum Electronics, World Scientific Publishing, Singapore, 2011.

[7] P. D. Drummond, M. S. Hillery, The Quantum Theory of Nonlinear Optics, Cambridge University Press, Cambridge, 2013.

[8] florian Kaiser, B. Fedrici, A. Zavatta, V. D'Auria, S. Tanzilli, A fully guided-wave approach to the generation and detection of squeezing at a telecom wavelength, in: Conference on Lasers and Electro-Optics, Optical Society of America, 2016, p. FF2C.2. doi:10.1364/CLEO_QELS.2016.FF2C.2.
URL http://www.osapublishing.org/abstract.cfm?URI=CLEO_QELS-2016-FF2C.2

[9] C. Reimer, M. Kues, L. Caspani, B. Wetzel, P. Roztocki, M. Clerici, Y. Jestin, M. Ferrera, M. Peccianti, A. Pasquazi, B. E. Little, S. T. Chu, D. J. Moss, R. Morandotti, Cross-polarized photon-pair generation and bi-chromatically pumped optical parametric oscillation on a chip, Nature Communications 6. doi:{10.1038/ncomms9236}.

[10] U. L. Andersen, T. Gehring, C. Marquardt, G. Leuchs, 30 years of squeezed light generation, Physica Scripta 91 (5) (2016) 053001.
URL http://stacks.iop.org/1402-4896/91/i=5/a=053001

[11] O. Alibart, V. D'Auria, M. D. Micheli, F. Doutre, F. Kaiser, L. Labonté, T. Lunghi, Éric Picholle, S. Tanzilli, Quantum photonics at telecom wavelengths based on lithium niobate waveguides, Journal of Optics 18 (10) (2016) 104001.
URL http://stacks.iop.org/2040-8986/18/i=10/a=104001

[12] M. J. Collins, C. Xiong, I. H. Rey, T. D. Vo, J. He, S. Shahnia, C. Reardon, T. F. Krauss, M. J. Steel, A. S. Clark, B. J. Eggleton, Integrated spatial multiplexing of heralded single-photon sources, Nat. Commun. 4 (2013) 2582–7. doi:10.1038/ncomms3582.
URL http://dx.doi.org/10.1038/ncomms3582

[13] R.-B. Jin, R. Shimizu, I. Morohashi, K. Wakui, M. Takeoka, S. Izumi, T. Sakamoto, M. Fujiwara, T. Yamashita, S. Miki, H. Terai, Z. Wang, M. Sasaki, Efficient generation of twin photons at telecom wavelengths with 2.5 GHz repetition-rate-tunable comb laser, SCIENTIFIC REPORTS 4. doi:{10.1038/srep07468}.

[14] S. Tanzilli, A. Martin, F. Kaiser, M. P. De Micheli, O. Alibart, D. B. Ostrowsky, On the genesis and evolution of integrated quantum optics, Laser Photon. Rev. 6 (1) (2012) 115–143. doi:10.1002/lpor.201100010.
URL http://dx.doi.org/10.1002/lpor.201100010

[15] P. Shadbolt, J. C. F. Mathews, A. Laing, J. L. O'Brien, Testing foundations of quantum mechanics with photons, Nature Physics 10 (4) (2014) 278–286. doi:10.1038/NPHYS2931.
URL http://dx.doi.org/10.1038/NPHYS2931

[16] A. Politi, M. J. Cryan, J. G. Rarity, S. Y. Yu, J. L. O'Brien, Silica-on-silicon waveguide quantum circuits, Science 320 (5876) (2008) 646–649. doi:10.1126/science.1155441.
URL http://dx.doi.org/10.1126/science.1155441

[17] S. Tanzilli, W. Tittel, H. De Riedmatten, H. Zbinden, P. Baldi, M. De Micheli, D. B. Ostrowsky, N. Gisin, PPLN waveguide for quantum communication, Eur. Phys. J. D 18 (2) (2002) 155–160. doi:10.1140/epjd/e20020019.
URL http://dx.doi.org/10.1140/epjd/e20020019

[18] C. Autebert, G. Boucher, F. Boitier, A. Eckstein, I. Favero, G. Leo, S. Ducci, Photon pair sources in AlGaAs: from electrical injection to quantum state engineering, J. Mod. Opt. 62 (20) (2015) 1739–1745. doi:10.1080/09500340.2014.1000412.
URL http://dx.doi.org/10.1080/09500340.2014.1000412

[19] C. Autebert, N. Bruno, A. Martin, A. Lemaitre, C. G. Carbonell, I. Favero, G. Leo, H. Zbinden, S. Ducci, Integrated AlGaAs source of highly indistinguishable and energy-time entangled photons, Optica 3 (2) (2016) 143–146. doi:10.1364/OPTICA.3.000143.
URL http://dx.doi.org/10.1364/OPTICA.3.000143

[20] J. E. Sharping, K. F. Lee, M. A. Foster, A. C. Turner, B. S. Schmidt, M. Lipson, A. L. Gaeta, P. Kumar, Generation of correlated photons in nanoscale silicon waveguides, Opt. Express 14 (25) (2006) 12388–12393. doi:10.1364/OE.14.012388.
URL http://dx.doi.org/10.1364/OE.14.012388

[21] Q. Lin, G. P. Agrawal, Silicon waveguides for creating quantum-correlated photon pairs, Opt. Lett. 31 (21) (2006) 3140–3142. doi:10.1364/OL.31.003140.
URL http://dx.doi.org/10.1364/OL.31.003140

[22] C. Xiong, B. Bell, B. Eggleton, Cmos-compatible photonic devices for single-photon generation, Nanophotonics 5 (3) (2016) 427–439.
URL doi:10.1515/nanoph-2016-0022

[23] M. J. Collins, A. S. Clark, J. K. He, D. Y. Choi, R. J. Williams, A. C. Judge, S. J. Madden, M. J. Withford, M. J. Steel, B. Luther Davies, C. L. Xiong, B. J. Eggleton, Low Raman-noise correlated photon-pair generation in a dispersion-engineered chalcogenide As_2S_3 planar waveguide, Opt. Lett. 37 (16) (2012) 3393–3395.
URL http://www.opticsinfobase.org/abstract.cfm?URI=ol-37-16-3393

[24] C. Xiong, L. G. Helt, A. C. Judge, G. D. Marshall, M. J. Steel, J. E. Sipe, B. J. Eggleton, Quantum-correlated photon pair generation in chalcogenide As_2S_3 waveguides, Opt. Express 18 (15) (2010) 16206–16216. doi:10.1364/OE.18.016206.
URL http://dx.doi.org/10.1364/OE.18.016206

[25] S. Azzini, D. Grassani, M. J. Strain, M. Sorel, L. G. Helt, J. E. Sipe, M. Liscidini, M. Galli, D. Bajoni, Ultra-low power generation of twin photons in a compact silicon ring resonator, Opt. Express 20 (21) (2012) 23100–23107. doi:10.1364/OE.20.023100.
URL http://dx.doi.org/10.1364/OE.20.023100

[26] N. C. Harris, D. Grassani, A. Simbula, M. Pant, M. Galli, T. Baehr-Jones, M. Hochberg, D. Englund, D. Bajoni, C. Galland, Integrated source of spectrally filtered correlated photons for large-scale quantum photonic systems, Phys. Rev. X 4 (4) (2014) 041047–10. doi:10.1103/PhysRevX.4.041047.
URL http://dx.doi.org/10.1103/PhysRevX.4.041047

[27] R. Kumar, J. R. Ong, M. Savanier, S. Mookherjea, Controlling the spectrum of photons generated on a silicon nanophotonic chip, Nat. Commun. 5 (2014) 5489–7. doi:10.1038/ncomms6489.
URL http://dx.doi.org/10.1038/ncomms6489

[28] E. Engin, D. Bonneau, C. M. Natarajan, A. S. Clark, M. G. Tanner, R. H. Hadfield, S. N. Dorenbos, V. Zwiller, K. Ohira, N. Suzuki, H. Yoshida, N. Iizuka, M. Ezaki, J. L. O'Brien, M. G. Thompson, Photon pair generation in a silicon micro-ring resonator with reverse bias enhancement, Opt. Express 21 (23) (2013) 27826–27834. doi:10.1364/OE.21.027826.
URL http://dx.doi.org/10.1364/OE.21.027826

[29] C. Xiong, C. Monat, A. S. Clark, C. Grillet, G. D. Marshall, M. J. Steel, J. T. Li, L. O'Faolain, T. F. Krauss, J. G. Rarity, B. J. Eggleton, Slow-light enhanced correlated photon pair generation in a silicon photonic crystal waveguide, Opt. Lett. 36 (17) (2011) 3413–3415.
URL http://www.opticsinfobase.org/abstract.cfm?URI=ol-36-17-3413

[30] J. K. He, A. S. Clark, M. J. Collins, J. T. Li, T. F. Krauss, B. J. Eggleton, C. L. Xiong, Degenerate photon-pair generation in an ultracompact silicon photonic crystal waveguide, Opt. Lett. 39 (12) (2014) 3575–3578. doi:10.1364/OL.39.003575.
URL http://dx.doi.org/10.1364/OL.39.003575

[31] J. L. O'Brien, A. Furusawa, J. Vuckovic, Photonic quantum technologies, Nature Photonics 3 (12) (2009) 687–695. doi:{10.1038/nphoton.2009.229}.

[32] C. Xiong, X. Zhang, A. Mahendra, J. He, D. Y. Choi, C. J. Chae, D. Marpaung, A. Leinse, R. G. Heideman, M. Hoekman, C. G. H. Roeloffzen, R. M. Oldenbeuving, P. W. L. van Dijk, C. Taddei, P. H. W. Leong, B. J. Eggleton, Compact and reconfigurable silicon nitride time-bin entanglement circuit, Optica 2 (8) (2015) 724–727. doi:10.1364/OPTICA.2.000724.
URL http://dx.doi.org/10.1364/OPTICA.2.000724

[33] D. Grassani, S. Azzini, M. Liscidini, M. Galli, M. J. Strain, M. Sorel, J. E. Sipe, D. Bajoni, Micrometer-scale integrated silicon source of time-energy entangled photons, Optica 2 (2) (2015) 88–94. doi:10.1364/OPTICA.2.000088.
URL http://www.osapublishing.org/optica/abstract.cfm?URI=optica-2-2-88

[34] C. Reimer, M. Kues, P. Roztocki, B. Wetzel, F. Grazioso, B. E. Little, S. T. Chu, T. Johnston, Y. Bromberg, L. Caspani, D. J. Moss, R. Morandotti, Generation of multiphoton entangled quantum states by means of integrated frequency combs, Science 351 (6278) (2016) 1176–1180. arXiv:http://science.sciencemag.org/content/351/6278/1176.full.pdf, doi:10.1126/science.aad8532.
URL http://science.sciencemag.org/content/351/6278/1176

[35] A. S. Solntsev, F. Setzpfandt, A. S. Clark, C. W. Wu, M. J. Collins, C. L. Xiong, A. Schreiber, F. Katzschmann, F. Eilenberger, R. Schiek, W. Sohler, A. Mitchell, C. Silberhorn, B. J. Eggleton, T. Pertsch, A. A. Sukhorukov, D. N. Neshev, Y. S. Kivshar, Generation of nonclassical biphoton states through cascaded quantum walks on a nonlinear chip, Phys. Rev. X 4 (3) (2014) 031007–13. doi:10.1103/PhysRevX.4.031007.
URL http://dx.doi.org/10.1103/PhysRevX.4.031007

[36] J. W. Silverstone, D. Bonneau, K. Ohira, N. Suzuki, H. Yoshida, N. Iizuka, M. Ezaki, C. M. Natarajan, M. G. Tanner, R. H. Hadfield, V. Zwiller, G. D. Marshall, J. G. Rarity, J. L. O'Brien, M. G. Thompson, On-chip quantum interference between silicon photon-pair sources, Nature Photonics 8 (2) (2014) 104–108. doi:10.1038/NPHOTON.2013.339.
URL http://dx.doi.org/10.1038/NPHOTON.2013.339

[37] H. Jin, F. M. Liu, P. Xu, J. L. Xia, M. L. Zhong, Y. Yuan, J. W. Zhou, Y. X. Gong, W. Wang, S. N. Zhu, On-chip generation and manipulation of entangled photons based on reconfigurable lithium-niobate waveguide circuits, Phys. Rev. Lett. 113 (10) (2014) 103601–5. doi:10.1103/PhysRevLett.113.103601.
URL http://dx.doi.org/10.1103/PhysRevLett.113.103601

[38] F. Setzpfandt, A. S. Solntsev, J. Titchener, C. W. Wu, C. L. Xiong, R. Schiek, T. Pertsch, D. N. Neshev, A. A. Sukhorukov, Tunable generation of entangled photons in a nonlinear directional coupler, Laser Photon. Rev. 10 (1) (2016) 131–136. doi:10.1002/lpor.201500216.
URL http://dx.doi.org/10.1002/lpor.201500216

[39] J. C. F. Matthews, A. Politi, A. Stefanov, J. L. O'Brien, Manipulation of multiphoton entanglement in waveguide quantum circuits, Nature Photonics 3 (6) (2009) 346–350. doi:10.1038/NPHOTON.2009.93.
URL http://dx.doi.org/10.1038/NPHOTON.2009.93

[40] A. Crespi, R. Ramponi, R. Osellame, L. Sansoni, I. Bongioanni, F. Sciarrino, G. Vallone, P. Mataloni, Integrated photonic quantum gates for polarization qubits, Nat. Commun. 2 (2011) 566–6. doi:10.1038/ncomms1570.
URL http://dx.doi.org/10.1038/ncomms1570

[41] D. Bonneau, E. Engin, K. Ohira, N. Suzuki, H. Yoshida, N. Iizuka, M. Ezaki, C. M. Natarajan, M. G. Tanner, R. H. Hadfield, S. N. Dorenbos, V. Zwiller, J. L. O'Brien, M. G. Thompson, Quantum interference and manipulation of entanglement in silicon wire waveguide quantum circuits, New J. Phys. 14 (2012) 045003–12. doi:10.1088/1367-2630/14/4/045003.
URL http://dx.doi.org/10.1088/1367-2630/14/4/045003

[42] R. Heilmann, M. Grafe, S. Nolte, A. Szameit, Arbitrary photonic wave plate operations on chip: Realizing hadamard, pauli-x, and rotation gates for polarisation qubits, Sci. Rep. 4 (2014) 4118–5. doi:10.1038/srep04118.
URL http://dx.doi.org/10.1038/srep04118

[43] T. Meany, M. Grafe, R. Heilmann, A. Perez-Leija, S. Gross, M. J. Steel, M. J. Withford, A. Szameit, Laser written circuits for quantum photonics, Laser Photon. Rev. 9 (4) (2015) 363–384. doi:10.1002/lpor.201500061.
URL http://dx.doi.org/10.1002/lpor.201500061

[44] A. Politi, J. C. F. Matthews, J. L. O'Brien, Shor's quantum factoring algorithm on a photonic chip, Science 325 (5945) (2009) 1221. doi:10.1126/science.1173731.
URL http://dx.doi.org/10.1126/science.1173731

[45] P. J. Shadbolt, M. R. Verde, A. Peruzzo, A. Politi, A. Laing, M. Lobino, J. C. F. Matthews, M. G. Thompson, J. L. O'Brien, Generating, manipulating and measuring entanglement and mixture with a reconfigurable photonic circuit, Nature Photonics 6 (1) (2012) 45–49. doi:10.1038/NPHOTON.2011.283.
URL http://dx.doi.org/10.1038/NPHOTON.2011.283

[46] A. Peruzzo, M. Lobino, J. C. F. Matthews, N. Matsuda, A. Politi, K. Poulios, X. Q. Zhou, Y. Lahini, N. Ismail, K. Worhoff, Y. Bromberg, Y. Silberberg, M. G. Thompson, J. L. O'Brien, Quantum walks of correlated photons, Science 329 (5998) (2010) 1500–1503. doi:10.1126/science.1193515.
URL http://dx.doi.org/10.1126/science.1193515

[47] M. A. Broome, A. Fedrizzi, S. Rahimi-Keshari, J. Dove, S. Aaronson, T. C. Ralph, A. G. White, Photonic boson sampling in a tunable circuit, Science 339 (6121) (2013) 794–798. doi:10.1126/science.1231440.
URL http://dx.doi.org/10.1126/science.1231440

[48] J. B. Spring, B. J. Metcalf, P. C. Humphreys, W. S. Kolthammer, X. M. Jin, M. Barbieri, A. Datta, N. Thomas-Peter, N. K. Langford, D. Kundys, J. C. Gates, B. J. Smith, P. G. R. Smith, I. A. Walmsley, Boson sampling on a photonic chip, Science 339 (6121) (2013) 798–801. doi:10.1126/science.1231692.
URL http://dx.doi.org/10.1126/science.1231692

[49] M. Tillmann, B. Dakic, R. Heilmann, S. Nolte, A. Szameit, P. Walther, Experimental boson sampling, Nature Photonics 7 (7) (2013) 540–544. doi:10.1038/NPHOTON.2013.102.
URL http://dx.doi.org/10.1038/NPHOTON.2013.102

[50] N. Spagnolo, C. Vitelli, M. Bentivegna, D. J. Brod, A. Crespi, F. Flamini, S. Giacomini, G. Milani, R. Ramponi, P. Mataloni, R. Osellame, E. F. Galvao, F. Sciarrino, Experimental validation of photonic boson sampling, Nature Photonics 8 (8) (2014) 615–620. doi:10.1038/NPHOTON.2014.135.
URL http://dx.doi.org/10.1038/NPHOTON.2014.135

[51] B. J. Metcalf, J. B. Spring, P. C. Humphreys, N. Thomas-Peter, M. Barbieri, W. S. Kolthammer, X. M. Jin, N. K. Langford, D. Kundys, J. C. Gates, B. J. Smith, P. G. R. Smith, I. A. Walmsley, Quantum teleportation on a photonic chip, Nature Photonics 8 (10) (2014) 770–774. doi:10.1038/NPHOTON.2014.217.
URL http://dx.doi.org/10.1038/NPHOTON.2014.217

[52] G. Corrielli, A. Crespi, R. Geremia, R. Ramponi, L. Sansoni, A. Santinelli, P. Mataloni, F. Sciarrino, R. Osellame, Rotated waveplates in integrated waveguide optics, Nat. Commun. 5 (2014) 4249–6. doi:10.1038/ncomms5249.
URL http://dx.doi.org/10.1038/ncomms5249

[53] C. Schaeff, R. Polster, R. Lapkiewicz, R. Fickler, S. Ramelow, A. Zeilinger, Scalable fiber integrated source for higher-dimensional path-entangled photonic qunits, Opt. Express 20 (15) (2012) 16145–16153. doi:10.1364/OE.20.016145.
URL http://www.opticsexpress.org/abstract.cfm?URI=oe-20-15-16145

[54] C. Schaeff, R. Polster, M. Huber, S. Ramelow, A. Zeilinger, Experimental access to higher-dimensional entangled quantum systems using integrated optics, Optica 2 (6) (2015) 523–529. doi:10.1364/OPTICA.2.000523.
URL http://www.osapublishing.org/optica/abstract.cfm?URI=optica-2-6-523

[55] F. Najafi, J. Mower, N. C. Harris, F. Bellei, A. Dane, C. Lee, X. L. Hu, P. Kharel, F. Marsili, S. Assefa, K. K. Berggren, D. Englund, On-chip detection of non-classical light by scalable integration of single-photon detectors, Nat. Commun. 6 (2015) 5873–8. doi:10.1038/ncomms6873.
URL http://dx.doi.org/10.1038/ncomms6873

[56] D. C. Burnham, D. L. Weinberg, Observation of simultaneity in parametric production of optical photon pairs, Phys. Rev. Lett. 25 (2) (1970) 84. doi:10.1103/PhysRevLett.25.84.
URL http://dx.doi.org/10.1103/PhysRevLett.25.84

[57] R. Schiek, A. S. Solntsev, D. N. Neshev, Temporal dynamics of all-optical switching in quadratic nonlinear directional couplers, Applied Physics Letters 100 (11). doi:http://dx.doi.org/10.1063/1.3696030.
URL http://scitation.aip.org/content/aip/journal/apl/100/11/10.1063/1.3696030

[58] R. Kruse, L. Sansoni, S. Brauner, R. Ricken, C. S. Hamilton, I. Jex, C. Silberhorn, Dual-path source engineering in integrated quantum optics, Phys. Rev. A 92 (5) (2015) 053841–6. doi:10.1103/PhysRevA.92.053841.
URL http://dx.doi.org/10.1103/PhysRevA.92.053841

[59] C. W. Wu, A. S. Solntsev, D. N. Neshev, A. A. Sukhorukov, Photon pair generation and pump filtering in nonlinear adiabatic waveguiding structures, Opt. Lett. 39 (4) (2014) 953–956. doi:10.1364/OL.39.000953.
URL http://dx.doi.org/10.1364/OL.39.000953

[60] A. S. Solntsev, A. A. Sukhorukov, D. N. Neshev, Y. S. Kivshar, Spontaneous parametric down-conversion and quantum walks in arrays of quadratic nonlinear waveguides, Phys. Rev. Lett. 108 (2) (2012) 023601–5. doi:10.1103/PhysRevLett.108.023601.
URL http://dx.doi.org/10.1103/PhysRevLett.108.023601

[61] M. Grafe, A. S. Solntsev, R. Keil, A. A. Sukhorukov, M. Heinrich, A. Tunnermann, S. Nolte, A. Szameit, Y. S. Kivshar, Biphoton generation in quadratic waveguide arrays: A classical optical simulation, Sci. Rep. 2 (2012) 562–5.

[62] A. S. Solntsev, A. A. Sukhorukov, D. N. Neshev, Y. S. Kivshar, Photon-pair generation in arrays of cubic nonlinear waveguides, Opt. Express 20 (24) (2012) 27441–27446. doi:10.1364/OE.20.027441.
URL http://www.opticsexpress.org/abstract.cfm?URI=oe-20-24-27441

[63] D. M. Markin, A. S. Solntsev, A. A. Sukhorukov, Generation of orbital-angular-momentum-entangled biphotons in triangular quadratic waveguide arrays, Phys. Rev. A 87 (2013) 063814. doi:10.1103/PhysRevA.87.063814.
URL http://link.aps.org/doi/10.1103/PhysRevA.87.063814

[64] D. A. Antonosyan, A. S. Solntsev, A. A. Sukhorukov, Single-photon spontaneous parametric down-conversion in quadratic nonlinear waveguide arrays, Optics Communications 327 (2014) 22 – 26, special Issue on Nonlinear Quantum Photonics. doi:http://dx.doi.org/10.1016/j.optcom.2014.02.047.
URL http://www.sciencedirect.com/science/article/pii/S0030401814001941

[65] D. Leykam, A. S. Solntsev, A. A. Sukhorukov, A. S. Desyatnikov, Lattice topology and spontaneous parametric down-conversion in quadratic nonlinear waveguide arrays, Phys. Rev. A 92 (2015) 033815. doi:10.1103/PhysRevA.92.033815.
URL http://link.aps.org/doi/10.1103/PhysRevA.92.033815

[66] F. Setzpfandt, A. A. Sukhorukov, D. N. Neshev, R. Schiek, A. S. Solntsev, R. Ricken, Y. Min, W. Sohler, Y. S. Kivshar, T. Pertsch, Spectral pulse transformations and phase transitions in quadratic nonlinear waveguide arrays, Opt. Express 19 (23) (2011) 23188–23201. doi:10.1364/OE.19.023188.
URL http://www.opticsexpress.org/abstract.cfm?URI=oe-19-23-23188

[67] F. Setzpfandt, A. S. Solntsev, D. N. Neshev, T. Pertsch, W. Sohler, R. Schiek, Temporal dynamics of spatially localized waves in quadratic nonlinear waveguide arrays, Phys. Rev. A 89 (2014) 033863. doi:10.1103/PhysRevA.89.033863.
URL http://link.aps.org/doi/10.1103/PhysRevA.89.033863

[68] J. G. Titchener, A. S. Solntsev, A. A. Sukhorukov, Generation of photons with all-optically-reconfigurable entanglement in integrated nonlinear waveguides, Phys. Rev. A 92 (3) (2015) 033819–12. doi:10.1103/PhysRevA.92.033819.
URL http://dx.doi.org/10.1103/PhysRevA.92.033819

[69] D. A. Antonosyan, A. S. Solntsev, A. A. Sukhorukov, Effect of loss on photon-pair generation in nonlinear waveguide arrays, Phys. Rev. A 90 (4) (2014) 043845–10. doi:10.1103/PhysRevA.90.043845.
URL http://dx.doi.org/10.1103/PhysRevA.90.043845

[70] R. Kruse, F. Katzschmann, A. Christ, A. Schreiber, S. Wilhelm, K. Laiho, A. Gabris, C. S. Hamilton, I. Jex, C. Silberhorn, Spatio-spectral characteristics of parametric down-conversion in waveguide arrays, New J. Phys. 15 (2013) 083046–24. doi:10.1088/1367-2630/15/8/083046.
URL http://dx.doi.org/10.1088/1367-2630/15/8/083046

[71] K. Garay-Palmett, A. B. U'Ren, R. Rangel-Rojo, R. Evans, S. Camacho-Lopez, Ultrabroadband photon pair preparation by spontaneous four-wave mixing in a dispersion-engineered optical fiber, Phys. Rev. A 78 (4) (2008) 043827–13. doi:10.1103/PhysRevA.78.043827.
URL http://dx.doi.org/10.1103/PhysRevA.78.043827

[72] J. W. Silverstone, R. Santagati, D. Bonneau, M. J. Strain, M. Sorel, J. L. O'Brien, M. G. Thompson, Qubit entanglement between ring-resonator photon-pair sources on a silicon chip, Nat. Commun. 6 (2015) 7948–7. doi:10.1038/ncomms8948.
URL http://dx.doi.org/10.1038/ncomms8948

[73] J. Lugani, S. Ghosh, K. Thyagarajan, Electro-optically switchable spatial-mode entangled photon pairs using a modified mach-zehnder interferometer, Opt. Lett. 37 (17) (2012) 3729–3731.
URL http://www.opticsinfobase.org/abstract.cfm?URI=ol-37-17-3729

[74] S. Clemmen, K. P. Huy, W. Bogaerts, R. G. Baets, P. Emplit, S. Massar, Continuous wave photon pair generation in silicon-on-insulator waveguides and ring resonators, Opt. Express 17 (19) (2009) 16558–16570. doi:10.1364/OE.17.016558.
URL http://dx.doi.org/10.1364/OE.17.016558

[75] C. Reimer, L. Caspani, M. Clerici, M. Ferrera, M. Kues, M. Peccianti, A. Pasquazi, L. Razzari, B. E. Little, S. T. Chu, D. J. Moss, R. Morandotti, Integrated frequency comb source of heralded single photons, Opt. Express 22 (6) (2014) 6535–6546. doi:10.1364/OE.22.006535.
URL http://dx.doi.org/10.1364/OE.22.006535

[76] X. Wang, W. Shi, H. Yun, S. Grist, N. A. F. Jaeger, L. Chrostowski, Narrow-band waveguide Bragg gratings on soi wafers with cmos-compatible fabrication process, Opt. Express 20 (14) (2012) 15547–15558. doi:10.1364/OE.20.015547.
URL http://dx.doi.org/10.1364/OE.20.015547

[77] M. Piekarek, D. Bonneau, S. Miki, T. Yamashita, M. Fujiwara, M. Sasaki, H. Terai, M. Tanner, C. M. Natarajan, R. H. Hadfield, jeremy o'brien, M. Thompson, Passive high-extinction integrated photonic filters for silicon quantum photonics, in: Conference on Lasers and Electro-Optics, Optical Society of America, 2016, p. FM1N.6. doi:10.1364/CLEO_QELS.2016.FM1N.6.
URL http://www.osapublishing.org/abstract.cfm?URI=CLEO_QELS-2016-FM1N.6

[78] M. Minkov, V. Savona, A compact, integrated silicon device for the generation of spectrally filtered, pair-correlated photons, J. Opt. 18 (5) (2016) 054012.
URL http://stacks.iop.org/2040-8986/18/i=5/a=054012

[79] F. Setzpfandt, M. Falkner, T. Pertsch, W. Sohler, R. Schiek, Bandstructure measurement in nonlinear optical waveguide arrays, Appl. Phys. Lett. 102 (8) (2013) 081104–4. doi:10.1063/1.4793565.
URL http://dx.doi.org/10.1063/1.4793565

[80] H. P. Chung, K. H. Huang, S. L. Yang, W. K. Chang, C. W. Wu, F. Setzpfandt, T. Pertsch, D. N. Neshev, Y. H. Chen, Adiabatic light transfer in titanium diffused lithium niobate waveguides, Opt. Express 23 (24) (2015) 30641–30650. doi:10.1364/OE.23.030641.
URL http://dx.doi.org/10.1364/OE.23.030641

[81] J. G. Titchener, A. S. Solntsev, A. A. Sukhorukov, Two-photon tomography using on-chip quantum walks, Opt. Lett. 41 (17) (2016) 4079–4082. doi:10.1364/OL.41.004079.
URL http://ol.osa.org/abstract.cfm?URI=ol-41-17-4079

[82] H. F. Hofmann, S. Takeuchi, Quantum phase gate for photonic qubits using only beam splitters and postselection, Phys. Rev. A 66 (2) (2002) 024308–3. doi:10.1103/PhysRevA.66.024308.
URL http://dx.doi.org/10.1103/PhysRevA.66.024308

[83] D. Gross, Y. K. Liu, S. T. Flammia, S. Becker, J. Eisert, Quantum state tomography via compressed sensing, Phys. Rev. Lett. 105 (15) (2010) 150401–4. doi:10.1103/PhysRevLett.105.150401.
URL http://dx.doi.org/10.1103/PhysRevLett.105.150401

[84] C. H. Baldwin, A. Kalev, I. H. Deutsch, Quantum process tomography of unitary and near-unitary maps, Phys. Rev. A 90 (1) (2014) 012110–10. doi:10.1103/PhysRevA.90.012110.
URL http://dx.doi.org/10.1103/PhysRevA.90.012110

[85] D. Oren, Y. Shechtman, M. Mutzafi, Y. C. Eldar, M. Segev, Sparsity-based recovery of three-photon quantum states from two-fold correlations, Optica 3 (3) (2016) 226–232. doi:10.1364/OPTICA.3.000226.
URL http://dx.doi.org/10.1364/OPTICA.3.000226

[86] R. Heilmann, J. Sperling, A. Perez-Leija, M. Grafe, M. Heinrich, S. Nolte, W. Vogel, A. Szameit, Harnessing click detectors for the genuine characterization of light states, Sci. Rep. 6 (2016) 19489–6. doi:10.1038/srep19489.
URL http://dx.doi.org/10.1038/srep19489

[87] M. Liscidini, J. E. Sipe, Stimulated emission tomography, Phys. Rev. Lett. 111 (19) (2013) 193602–5. doi:10.1103/PhysRevLett.111.193602.
URL http://dx.doi.org/10.1103/PhysRevLett.111.193602

[88] A. Eckstein, G. Boucher, A. Lemaitre, P. Filloux, I. Favero, G. Leo, J. E. Sipe, M. Liscidini, S. Ducci, High-resolution spectral characterization of two photon states via classical measurements, Laser Photon. Rev. 8 (5) (2014) L76–L80. doi:10.1002/lpor.201400057.
URL http://dx.doi.org/10.1002/lpor.201400057

[89] I. Jizan, L. G. Helt, C. L. Xiong, M. J. Collins, D. Y. Choi, C. J. Chae, M. Liscidini, M. J. Steel, B. J. Eggleton, A. S. Clark, Bi-photon spectral correlation measurements from a silicon nanowire in the quantum and classical regimes, Sci. Rep. 5 (2015) 12557–9. doi:10.1038/srep12557.
URL http://dx.doi.org/10.1038/srep12557

[90] L. A. Rozema, C. Wang, D. H. Mahler, A. Hayat, A. M. Steinberg, J. E. Sipe, M. Liscidini, Characterizing an entangled-photon source with classical detectors and measurements, Optica 2 (5) (2015) 430–433. doi:10.1364/OPTICA.2.000430.
URL http://dx.doi.org/10.1364/OPTICA.2.000430

[91] L. G. Helt, M. J. Steel, J. E. Sipe, Spontaneous parametric downconversion in waveguides: what's loss got to do with it?, New J. Phys. 17 (2015) 013055–17. doi:10.1088/1367-2630/17/1/013055.
URL http://dx.doi.org/10.1088/1367-2630/17/1/013055

[92] L. G. Helt, M. J. Steel, Effect of scattering loss on connections between classical and quantum processes in second-order nonlinear waveguides, Opt. Lett. 40 (7) (2015) 1460–1463. doi:10.1364/OL.40.001460.
URL http://dx.doi.org/10.1364/OL.40.001460

[93] F. Lenzini, J. Titchener, S. Kasture, A. Poddubny, A. Boes, B. Haylock, M. Villa, A. Mitchell, A. S. Solntsev, A. A. Sukhorukov, M. Lobino, A nonlinear waveguide array with inhomogeneous poling pattern for the generation of photon pairs, in: Conference on Lasers and Electro-Optics, Optical Society of America, 2016, p. FTh4A.1. doi:10.1364/CLEO_QELS.2016.FTh4A.1.
URL http://www.osapublishing.org/abstract.cfm?URI=CLEO_QELS-2016-FTh4A.1

[94] A. N. Poddubny, I. V. Iorsh, A. A. Sukhorukov, Generation of photon-plasmon quantum states in nonlinear hyperbolic metamaterials, Phys. Rev. Lett. 117 (2016) 123901. doi:10.1103/PhysRevLett.117.123901.
URL http://link.aps.org/doi/10.1103/PhysRevLett.117.123901

[95] L. Sansoni, K. H. Luo, R. Ricken, S. Krapick, H. Herrmann, C. Silberhorn, A two-channel source of spectrally degenerate polarization entangled states on chip, in: Conference on Lasers and Electro-Optics, Optical Society of America, 2016, p. FM2N.2. doi:10.1364/CLEO_QELS.2016.FM2N.2.
URL http://www.osapublishing.org/abstract.cfm?URI=CLEO_QELS-2016-FM2N.2

[96] A. Rossi, G. Vallone, A. Chiuri, F. De Martini, P. Mataloni, Multipath entanglement of two photons, Phys. Rev. Lett. 102 (15) (2009) 153902–4. doi:10.1103/PhysRevLett.102.153902.
URL http://dx.doi.org/10.1103/PhysRevLett.102.153902

[97] R. Ceccarelli, G. Vallone, F. De Martini, P. Mataloni, A. Cabello, Experimental entanglement and nonlocality of a two-photon six-qubit cluster state, Phys. Rev. Lett. 103 (16) (2009) 160401–4. doi:10.1103/PhysRevLett.103.160401.
URL http://dx.doi.org/10.1103/PhysRevLett.103.160401

[98] M. F. Saleh, G. Di Giuseppe, B. E. A. Saleh, M. C. Teich, Modal and polarization qubits in ti:$LiNbO_3$ photonic circuits for a universal quantum logic gate, Opt. Express 18 (19) (2010) 20475–20490.
URL http://www.opticsinfobase.org/abstract.cfm?URI=oe-18-19-20475

[99] A. Gatti, T. Corti, E. Brambilla, D. B. Horoshko, Dimensionality of the spatiotemporal entanglement of parametric down-conversion photon pairs, Phys. Rev. A 86 (5) (2012) 053803–12. doi:10.1103/PhysRevA.86.053803.
URL http://dx.doi.org/10.1103/PhysRevA.86.053803